



Statistics of Bicycle Rider Motion

Jason K. Moore^{a,*}, Mont Hubbard^a, A. L. Schwab^b, J. D. G. Kooijman^b, Dale L. Peterson^a

^a*Sports Biomechanics Lab, University of California, Davis, Davis, CA, USA, 95616*

^b*Laboratory for Engineering Mechanics, Delft University of Technology, Mekelweg 2, 2628CD Delft, The Netherlands*

Abstract

An overview of bicycle and rider kinematic motions from a series of experimental treadmill tests is presented. The full kinematics of bicycles and riders were measured with an active motion capture system. Motion across speeds are compared graphically with box and whiskers plots. Trends and ranges in amplitude are shown to characterize the system motion. This data will be used to develop a realistic biomechanical model and control model for the rider and for future experimental design. © 2010 Published by Elsevier Ltd.

Keywords:

bicycle dynamics, human control, motion capture, experiments, statistics

1. Introduction

In the past decade, research has grown on single track vehicles culminating in the recently benchmarked bicycle model [1]. Two other recent papers [2, 3] have also presented overviews of current and historical research in bicycle dynamics and control. These review a plethora of dynamic models but little is known about which models are good at representing the actual system. Very little model-validation experimentation has been performed in the literature and many of the modeling assumptions, especially those regarding tire and rider dynamics, remain questionable. The most recent notable model-validation study is the verification of the benchmark model [4]. Only a handful of other good experimental studies on bicycle dynamics exist. The work [5] performed some 40 years ago in the same halls as the Kooijman experiments [4] included extensive efforts to validate a human control model using a bicycle simulator paired with statistical analysis. Also, around the same time as the first Delft experiments [5], a substantial study was done at Calspan and Schwinn [6].

With these studies providing some background, we have begun work to validate the kinematics of the bicycle and rider in a way that can facilitate the derivation of both dynamic models of

*Corresponding author. Tel.: +01(530)752-2163

Email address: moorepants@gmail.com (Jason K. Moore)

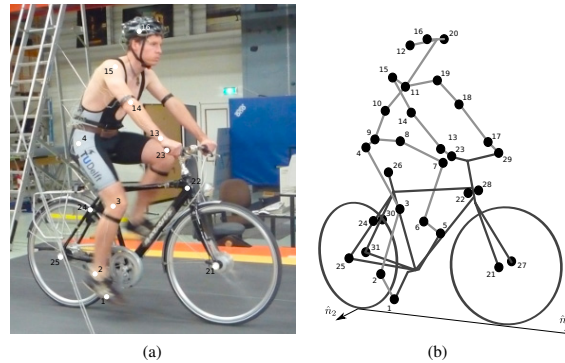


Figure 1: (a) Rider 1 on one of the two bicycles with marker positions. (b) Schematic of the marker positions.

the bike and rider and a rider control model. Our work began with an instrumented bicycle [7] that was capable of measuring dynamics and collecting video of the rider's motion. We then used full body motion capture [8] to quantitatively characterize the rider and bicycle kinematics. Principal component analysis was used to analyze the motion capture data but this proved to give less insight than expected. These initial efforts did show that the dominant motions for control are steering, that the rider's motions are small for normal bicycling tasks, and that pedaling motions are correlated with other rider motions. The present work examines the same motion capture data from [8] with rigid body kinematics in mind and uses a statistical approach to identify trends with forward speed, a strong dependency of bicycle stability.

2. Experimental Design

The experiments were performed in a controlled environment while the motion of the bicycle and rider were measured with an active motion capture system [9]. The rider rode on a 3×5 meter treadmill, (Fig. 1) capable of belt speeds up to 35 km/h. Three male riders of similar age [23, 26, 31 years] and build [height (1.84, 1.83, 1.76 m) and mass (74, 72, 72 kg)] participated as subjects. Each rode two different Dutch bicycles. Each rider performed all runs in one day in the same order (no randomization) and was instructed to bicycle comfortably at a constant speed in the range of 2 to 30 km/h for the duration of the run. There were at least 2 repetitions of each speed with each bicycle. A run was sampled at a frequency of 100 Hz for 60 seconds.

Bicycle markers were placed to easily extract the rigid body motion (i.e. body orientations and locations) of the frame and fork (Fig. 1). Four markers were attached to the fork and seven to the rear frame. A marker was attached on the right and left sides of the center of each wheel, the seat stays, the ends of the handlebars, and the head tube. A single marker was also attached to the back of the seat post.

We recorded the locations of 20 points on the rider (Fig. 1): left and right sides of the helmet near the temple, back of the helmet, shoulders (greater tuberosity of the humerus), elbows (lateral

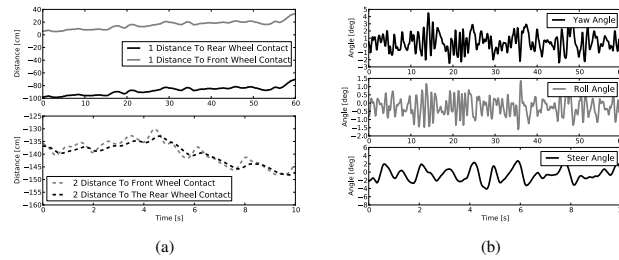


Figure 2: Time histories of various bicycle rigid body generalized coordinates for a normal biking run at 10 km/h. (a) Positions of the wheel contacts in the \hat{n}_1 and \hat{n}_2 directions (Fig. 1b). (b) Bicycle yaw, roll and steer angles.

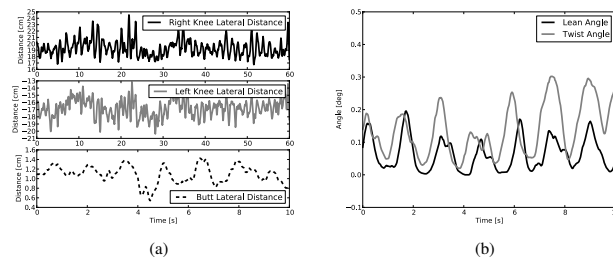


Figure 3: Time histories of various rider rigid body generalized coordinates for a normal biking run at 10 km/h. (a) Lateral deviations of the knees and butt from the frame plane. (b) Rider lean and twist angles.

epicondyle of the humerus), wrists (pisiform of the carpus), between the shoulder blades on the spine (T6 of the thoracic vertebrae), the tail bone (coccyx), midpoint on the spine between the coccyx and shoulder blades (L1 on the lumbar vertebrae), hips (greater trochanter of the femur), knees (lateral epicondyle of the femur), ankles (lateral malleolus of the fibula) and feet (proximal metatarsal joint).

3. Results

Once marker data was repaired, we calculated several generalized coordinates. This provided a way to characterize the bicycle and rider as a system of rigid bodies which seems to give a clearer picture of the underlying control motions that the principal component analysis provided [8]. The coordinates included bicycle yaw, roll and steer angles and the locations of the wheel ground contact points, and several coordinates to represent rider motion: the rider's

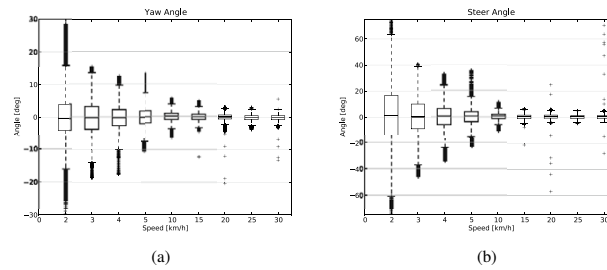


Figure 4: Box and whiskers plots of the coordinate data from all riders and bicycles versus speed; (a) yaw angle and (b) steer angle.

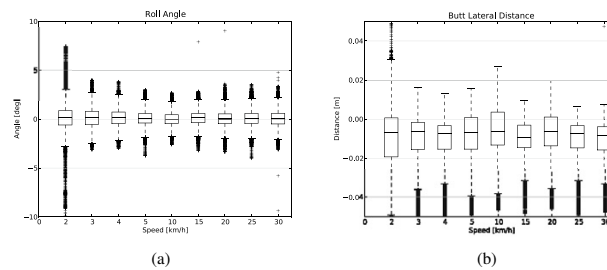


Figure 5: Box and whiskers plots of the coordinate data from all riders and bicycles versus speed; (a) roll angle and (b) lateral butt distance.

lean and twist angles, lateral knee motion, and lateral tail bone motion, all relative to the bicycle frame plane of symmetry. The rider lean angle can be thought of as the angle of the rider's spine relative to the bicycle frame. The twist is the angle through which the torso rotates about the spine. The knee and butt motions are the relative lateral distances from the frame plane of symmetry for each marker. These are shown because we observed large lateral knee movement in video footage at low speeds [7] that may be used for additional control. The butt motion is plotted to give an idea of how the seat can potentially be shifted under the torso to control roll angle. Figures 2 and 3 show typical time histories of these coordinates.

Little can be determined from the time histories alone (there are nearly 3000 different time histories to examine) beyond some slight correlations in frequency patterns. Examining the frequency spectrum of each time history gives a different and more revealing view. The pedaling frequency typically appears in each coordinate frequency but no other distinct frequencies stand out [8].

A better way to visualize how the coordinates change with speed, for example, is to look at statistical distributions of the time histories. We grouped all of the runs together for combined

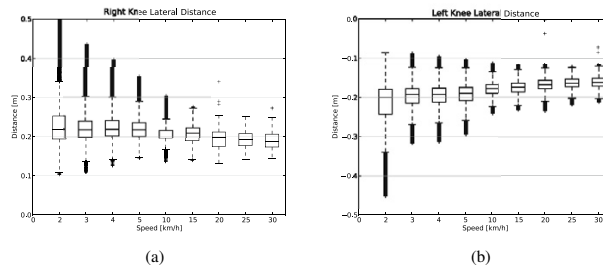


Figure 6: Box and whiskers plots of the lateral distance data from all rider and bicycles versus speed; (a) right knee and (b) left knee.

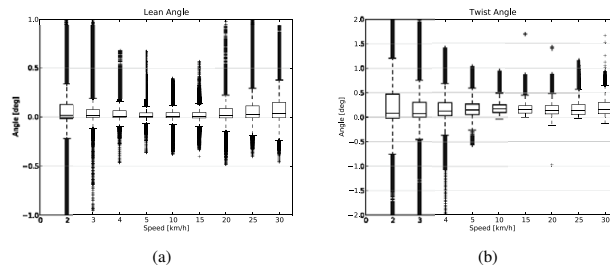


Figure 7: Box and whiskers plots of the data from all riders and bicycles versus speed; (a) lean angle and (b) twist angle.

data sets at each speed of between 48,000 and 72,000 points, depending on how many repetitions of runs were performed (i.e. between 8 and 12). These were then plotted as separate box plots for each speed and for each state, Figures 4, 5, and 6, 7. The box and whiskers charts plot a center line for the median of the data, a box that bounds the 25% and 75% quartiles, whiskers that encompass the data that falls within $1.5 \times (Q_{75} - Q_{25})$ and crosses for any outlier data points. Trends can be identified based on the spread and median of the data at each speed. An offset median shows that the distribution is skewed (e.g. steering more to the left than the right). The box and the whiskers encompass the vast majority of the data. The whiskers can be used to compare the coordinate excursions across speeds.

The yaw and steer plots show that the angles are small and tightly distributed at high speeds, but that below 10 km/h the spread begins to grow. It is also interesting that the yaw and steer graphs have very similar distributions. For a bicycle without a rider, there is a simple kinematic relationship such that yaw rate is only a function of steer rate and steer angle. If this holds true in the experimental data, then there is probably little influence of other body motions in the steer and yaw coordinates. The spread of the roll angle on the other hand stays fairly constant regardless

of speed. The butt lateral distance has somewhat constant distributions across speeds and it is also apparent that the rider is sitting about one centimeter off the center plane of the bicycle. The lateral knee distances are interesting in the fact that spreads increase with lower speeds. We were able to visually detect large knee movements in the video data at low speeds and hypothesized about the role the knees could possibly play in control of the bicycle [7, 8]. The rider lean angles are very small and do not show much change with speed but the rider twist angles show a little more spread at low speeds.

4. Conclusions

The box and whiskers plots are a method of visualizing a statistically valid view of the kinematics of the bicycle and rider during stabilization tasks. General trends in how states change with speed were shown and can be utilized for rider bicycle dynamic and control model design. The numerical values presented also provide a framework for design of measurement techniques needed in experimental studies. Future work will include expanding this to rates, accelerations and the frequency content of the signals. These can then be compared statistically for significant differences across speeds, bikes, riders and riding tasks.

References

- [1] J. P. Meijaard, J. M. Papadopoulos, A. Ruina, A. L. Schwab, Linearized dynamics equations for the balance and steer of a bicycle: A benchmark and review, *Proceedings of the Royal Society A: Mathematical, Physical and Engineering Sciences* 463 (2084) (2007) 1955–1982. doi:10.1098/rspa.2007.1857.
URL <http://rspa.royalsocietypublishing.org/content/463/2084/1955.abstract>
- [2] K. J. Åström, R. E. Klein, A. Lennartsson, Bicycle dynamics and control, *IEEE Control Systems Magazine* 25 (4) (2005) 26–47. doi:10.1109/MCS.2005.1499389.
- [3] D. J. Limebeer, R. S. Sharp, Bicycles, motorcycles, and models, *IEEE Control Systems Magazine* 26 (5) (2006) 34–61.
- [4] J. D. G. Kooijman, A. L. Schwab, J. P. Meijaard, Experimental validation of a model of an uncontrolled bicycle, *Multibody System Dynamics* 19 (2008) 115–132. doi:10.1007/s11044-007-9050-x.
- [5] A. van Lunteren, H. G. Stassen, Investigations on the bicycle simulator, Chapter III of Annual Report 1969 of the Man-Machine Systems Group WTHD21, Delft University of Technology, Laboratory for Measurement and Control (1970).
- [6] R. D. Roland Jr., D. E. Massing, A digital computer simulation of bicycle dynamics, Calspan Report YA-3063-K-1, Cornell Aeronautical Laboratory, Inc., Buffalo, NY, 14221, prepared for Schwinn Bicycle Company, Chicago, IL 60639 (June 1971).
- [7] J. D. G. Kooijman, A. L. Schwab, J. K. Moore, Some observations on human control of a bicycle, in: *Proceedings of the ASME 2009 International Design and Engineering Technical Conferences & Computers and Information in Engineering Conference*, 2009.
- [8] J. K. Moore, J. D. G. Kooijman, A. L. Schwab, Rider motion identification during normal bicycling by means of principal component analysis, in: K. Arczewski, M. W. J. Frączek (Eds.), *Multibody Dynamics 2009, ECCOMAS Thematic Conference*, Warsaw, Poland, 2009.
- [9] Northern Digital Incorporated, Optotrak Certus Motion Capture System (2009).
URL <http://www.ndigital.com/>